



A novel water hyacinth based biosorbent for 2,4-dichlorophenoxyacetic acid (2,4-D) removal from aqueous solution

M.T. Aswani, M.V. Pavan Kumar*

Department of Chemical Engineering, National Institute of Technology Calicut, Kozhikode-673601, India,
email: aswanishok976@gmail.com (M.T. Aswani), malladi@nitc.ac.in (M.V. Pavan Kumar)

Received 4 February 2019; Accepted 16 June 2019

ABSTRACT

In the current study, a novel low cost biosorbent was developed using water hyacinth root powder for the biosorption of a phenoxy pesticide (2,4-dichlorophenoxy acetic acid) from its aqueous solution. Initially, biosorbents were prepared by systematically modifying the water hyacinth root powder with acid, thermal, ultrasound, thermal-acid and ultrasound-acid treatments. The ultrasound-acid modified biosorbent exhibited superior biosorption capacity over the others with a maximum biosorption capacity of 40.0 mg g⁻¹. For the ultrasound-acid treated biosorbent, three biosorption operation parameters namely biosorbent dosage, solution pH and initial pesticide concentration were varied to obtain their optimal values for maximum biosorption capacity. A maximum removal of 91% was obtained for 4 g L⁻¹ dosage of ultrasound-acid modified biosorbent at pH of 4 in 100 mg L⁻¹ of the pesticide solution. The presence of various sulphur containing functional groups on the surface of ultrasound-acid treated biosorbent might be the reason for the enhanced biosorption capacity. The biosorption kinetic data obtained for different initial concentrations with the optimal values of biosorbent dosage and pH were well fitted to pseudo second order kinetic model indicating chemisorption type interaction. The biosorption equilibrium data was well fitted to Langmuir isotherm model which represent mono layered biosorption. The presence of intra particle and film diffusion limitations for the biosorption were confirmed using two well-known intra particle diffusion models namely Weber and Boyd.

Keywords: Biosorption; Biosorption kinetics; Biosorption isotherm; Water Hyacinth Root Powder; 2,4-dichlorophenoxy acetic acid; Pesticide

1. Introduction

The extensive agriculture and cultivation to full fill the requirements of exponentially growing population have resulted in the increased usage of pesticides leading to serious water contamination. The presence of pesticide residues mainly chlorophenols in water bodies can pose serious damage to ecosystems. 2,4-dichlorophenoxy acetic acid (2,4-D) is a phenoxy compound and an important one among chlorinated pesticides. It is widely used as a systemic herbicide for the selective removal of various types of broad leaf weeds found in different crops [1]. 2,4-D is a toxic, poorly biodegradable and an essential

component in many herbicide mixtures. The half-life of 2,4-D is dependent on the natural sources where it is accumulated. Under aerobic conditions, the half-life of 2,4-D in water varies from days to many weeks. On the other hand, the half-life of 2,4-D in water is more than 120 days under anaerobic conditions [2,3]. The solubility of 2,4-D in water is 900 mg L⁻¹ [4] and the maximum acceptable limit of 2,4-D in potable water is 100 ppb [5]. However, studies indicated that 2,4-D can damage human cells and causes cancer. Considering the health risks of 2,4-D, it is very essential to find out techniques to separate the same from contaminated waters.

Due to its selectivity, cost efficiency and effectiveness at lower contaminant concentrations, adsorption is considered to be a suitable method over the other available

*Corresponding author.

methods (photochemical degradation, membrane filtration, coagulation etc.) for the removal of dyes, heavy metals and pesticides like 2,4-D from environmental matrices [6–8]. Generally, activated carbons and synthetic resins are vividly used as adsorbents due to favourable characteristics such as high surface area, porosity and presence of different functional groups. However, these materials are not much viable due to high preparation costs, especially when they are derived from non-renewable sources. Thus, the development of low cost and efficient biosorbents using renewable and easily available biomass has received great attention in the last decade [9]. Moreover, the removal of pesticides using various low cost biosorbents is a novel research topic now [10].

Water Hyacinth (WH) is an invasive, rapidly growing and multiplying aquatic weed which is highly tolerant to pollution [11]. It is regarded as an extreme threat to ecological balance in and around water bodies [12]. Earlier, WH biomass was shown to be an effective biosorbent for the removal of different types of heavy metals and dyes [13,14]. The development of low cost WH based biosorbents can be considered as an option because of the abundance of WH in aquatic systems as waste biomass [15].

Nevertheless, WH based biomass has not been extensively explored for the removal of harmful pesticides such as 2,4-D. To the best of our knowledge, this is the first work reporting different physical and chemical modifications of Water Hyacinth Root Powder (WHRP) and testing the modified biosorbents for the removal of pesticide 2,4-D. In this study, ultrasound-acid modification of virgin biosorbent was found to be suitable for favourable biosorption of 2,4-D. Different characterization techniques were performed to study the thermal stability, specific surface area, morphology and the presence of various functional groups on the biosorbent surface. For the ultrasound-acid modified biosorbent, the optimal values of biosorbent dosage, solution *pH* and initial pesticide concentration were obtained experimentally. The experimental data was fitted for different kinetics and equilibrium models. The ultrasound-acid modification of WH biosorbent was found to be suitable for 2,4-D biosorption.

2. Materials and methods

2.1. Adsorbate

The analytical grade 2,4-D of 97% purity was purchased from Sigma Aldrich (USA) and the standard stock solutions were prepared by dissolving the pesticide in millipore water. Using this stock solution, solutions of required 2,4-D concentrations were prepared by appropriate series of dilutions. The general characteristics of 2,4-D are listed in Table S1 (supplementary data).

2.2. Preparation and modification of biosorbent

WH plants were grown in an artificial cultivation pond. The roots were separated and washed with distilled water. The cleaned roots were dried at 105°C for 24 h followed by grinding. The resultant powder was used as the base material for the preparation of modified bio-

sorbents. The WHRP was broadly modified in three different ways as shown in Table 1 (physical, chemical and physicochemical).

2.2.1. Physical modification

In case of physical modifications, the first one (thermal treatment) was carried out in a muffle furnace at three different temperatures (300, 500, 700°C) with no external air or gas supply for 3 h. The yields of obtained chars at 300, 500 and 700°C were 67%, 56% and 22% respectively. In the second method of physical modification, the powders were ultrasonicated (20 amplitude) for three different time intervals (15, 30, 60 min) separately, followed by water wash and drying for one day at 70°C. The prepared biosorbents by physical modifications were tested directly for the biosorption of 2,4-D.

2.2.2. Chemical modification

Here, solutions of aqueous sulphuric acid of three different concentrations (4, 6, 10 (v/v) %) were employed. In each case, 2 g of WHRP was incubated in the corresponding acid solution for one day, 100 rpm at 30°C followed by washing with distilled water. The treated WHRPs were dried at 70°C for 24 h and later tested for the biosorption of 2,4-D.

2.2.3. Physicochemical modification

Two different types of physicochemical modifications namely thermal-acid treatment and ultrasound-acid treatment were employed for the raw biosorbent, i.e., WHRP. In both methods, the optimized sulphuric acid concentration (6%, v/v) that was found in the chemical modification for the removal of 2,4-D was used. In the first physicochemical modification, the thermally treated (300, 500, 700°C) powders of WHRP were acid modified using 6% (v/v) sulphuric acid solution followed by washing and drying (70°C for 24 h). In the second physicochemical modification, WHRP is ultrasonicated for three different durations (15, 30, 60 min) separately in the optimized concentration of sulphuric acid solution. The treated biosorbents were washed and dried as mentioned above. The treatment conditions are given in Table 1.

Table 1
Modifications of WHRP

Type of modification	Method of modification	Conditions
Physical	Thermal	300°C, 500°C, 700°C
	Ultra sonication	15, 30, 60 min
Chemical	Acid treatment	4, 6, 10 (v/v) %, H ₂ SO ₄
Physicochemical	Thermal + Acid (one after the other)	300, 500, 700°C + 6 (v/v) %, H ₂ SO ₄
	Ultra sonication + Acid (together)	15, 30, 60 min, + 6 (v/v) %, H ₂ SO ₄

2.3. Characterization of biosorbent

The surfaces of selected biosorbents were analysed using Fourier Transform Infrared (FT-IR) spectrometer (Cary 630, Agilent technologies, Malaysia) in the range of 4000–400 cm^{-1} to know about various functional groups present on the biosorbents surfaces. Thermal characteristics of selected biosorbents were tested using Thermo Gravimetric Analyser (TGA) in the range of 30–900°C with a heating rate 10°C min^{-1} in nitrogen/inert atmosphere (STA7200, Hitachi, Japan). The surface topography was analysed using Scanning Electron Microscopy (SEM) analyser (JEOL Model JSM-6390LV, Japan). The specific surface areas of selected biosorbents were estimated using Micromeritics ASAP 2020 Porosimeter using Brunauer Emmett Teller (BET) isotherm model.

2.4. Batch biosorption studies

The batch biosorption studies were performed (till attaining equilibrium) in 100 mL beakers with 50 mL solution of 100 mg L^{-1} pesticide concentration with a stirring rate of 250 rpm (magnetic stirrer) at native solution *pH*. After identifying the biosorbent for the maximum removal of 2,4-D, the effect of different parameters such as biosorbent dosage, initial *pH* of solution and initial solution concentrations on the removal of 2,4-D were studied for the same biosorbent and the optimal operating values were obtained in sequential manner. Three different dosages (2, 4, 6 g L^{-1}) were tested for this purpose. The influence of solution *pH* on biosorption was studied in the *pH* range of 2–11. The *pH* of the solution was adjusted using 0.1 M HCl and 0.1 M NaOH. Using a stock solution of 2,4-D (500 mg L^{-1}), different solutions with concentrations in the range of 20–180 mg L^{-1} were prepared to study the effect of initial concentration on the 2,4-D biosorption. The samples were carefully collected from each batch experiment at regular time intervals, centrifuged at 4500 rpm for 10 min and tested for the pesticide concentration using double beam UV-Vis spectropho-

tometer (Perkin-Elmer Lambda 650, USA) at 284 nm [8]. The amount of pesticide (q_t , mg g^{-1}) biosorbed and percentage of pesticide removal (*R*) at time *t* (min) were calculated by Eq. (1) and Eq. (2) [16]:

$$q_t = \frac{(C_o - C_t)V}{W} \quad (1)$$

$$R\% = \frac{(C_o - C_t)}{C_o} 100 \quad (2)$$

where C_o and C_t (mg L^{-1}) represent initial concentration and concentration at time *t*, respectively. *W* (g) is the amount of biosorbent used and *V* is the total volume of pesticide solution in L.

3. Results and discussion

3.1. Effect of biosorbent modification

Initially, the unmodified (WHRP) and modified biosorbents were tested under batch mode at native *pH* and room temperature. Fig. 1a shows that the acid treatment alone significantly improves the biosorption characteristics of virgin root powder. A maximum of 70% removal of 2,4-D was seen with the acid modification of WHRP biosorbent with 6% H_2SO_4 solution. The percentage of removal of 2,4-D with 10% H_2SO_4 solution treated biosorbent is 66. This decrease in biosorption capacity might be due to the structural changes of active functional groups present on the surface of biosorbent. The modification of biosorbent with higher concentration of H_2SO_4 may result in the decrease of solution *pH* during batch biosorption leading to lesser uptake of 2,4-D.

The thermal treatment alone or its combination with acid treatment of WHRP could not exhibit favourable biosorption characteristics as shown in Fig. 1b. The thermal

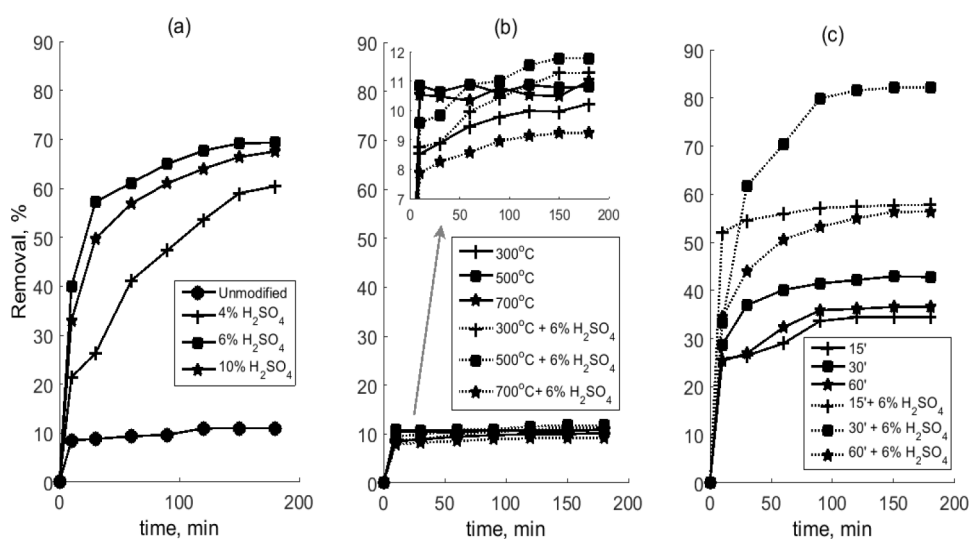


Fig. 1. Biosorption of 2,4-D by water hyacinth root biosorbents: (a) acid treated, (b) thermal and thermal-acid treated (c) ultrasonicated and ultrasound-acid treated (biosorbent dosage: 2 g L^{-1} , initial 2,4-D solution concentration: 100 mg L^{-1} , Exposure time: 3 h, stirring speed: 250 rpm at native *pH*).

treatment at higher temperatures may destruct the surface structure and internal pore channels. These changes can potentially reduce the uptake of adsorbate during biosorption.

A maximum of 82% removal of 2,4-D was seen in the batch biosorption experiments with ultrasound-acid modified biosorbent (6% H_2SO_4 solution, 30 min) as shown in Fig. 1c. The equilibrium percentage removal for ultrasound-acid treated biosorbent of 15 and 60 min of sonication are 56 and 54 respectively. Increase of treatment time to 60 min can change the biosorbent structure and reduce the available active sites for the biosorption.

Note that the unmodified biosorbent and thermal-acid treated biosorbent exhibited poor biosorption characteristics as shown in Figs. 1a and 1b. As ultrasound-acid modification (6% H_2SO_4 , 20A, 30 min) of the biosorbent yielded to the highest biosorption capacity, further batch studies were performed using this ultrasound-acid modified biosorbent to identify optimal biosorbent dosage, *pH* and initial concentration sequentially. Overall, the acid treatment has a significant positive effect on the biosorption characteristics for the WHRP.

3.2. Characterization of biosorbents

The characterisation of biosorbent materials is vital to correlate their properties with the observed biosorption efficiencies. The characterization studies were carried out on unmodified, acid modified (6% H_2SO_4 , 30 min) and ultrasound-acid modified (6% H_2SO_4 , 20A, 30 min) biosorbents.

3.2.1. FT-IR analysis

The FT-IR spectra of the three different WHRP biosorbents (unmodified, acid modified and ultrasound-acid modified) are shown in Fig. 2a. The broad peak around 3355 cm^{-1} reveals the occurrence of -OH and -NH stretching of hydroxyl and amine groups respectively on the surface [17]. The peaks at 2919 cm^{-1} , 2115 cm^{-1} and 1710 cm^{-1} are assigned to -CH stretch, C=C bonds and C=O stretches

respectively. High intensity peak observed at 1680 cm^{-1} represents C=O stretch in the case of unmodified WHRP. With ultrasound-acid modification, the C=O stretch peak at 1680 cm^{-1} got weakened. Besides, two new bonds viz., C-O stretch and -SOH symmetric bend at 1020 cm^{-1} [17] and 1136 cm^{-1} respectively appeared. In the case of acid treated biosorbent, the above peaks are present but with very low intensities. In case of ultrasound-acid modified biosorbent, two peaks at 884 cm^{-1} and 565 cm^{-1} indicate -S(OH)₂ asymmetric stretch and O-S=O bond respectively [18]. These two peaks are not present for the acid treated biosorbent. The FT-IR analysis results are tabulated in Table S2 (supplementary data). The significant difference between unmodified biosorbent and biosorbent with ultrasound-acid modification is the presence of the functional groups containing sulphur in the latter.

3.2.2. Thermo gravimetric analysis (TGA)

The thermo gravimetric analysis of biosorbents is presented in Fig. 2b. The weight loss in all cases till 100°C is attributed to the removal of physically adsorbed moisture [19]. In case of unmodified biosorbent, the observed loss of weight in the range of $270\text{--}390^\circ\text{C}$ was due to volatilization of cellulose and hemicellulose [20]. The next stage of weight loss in the range of $390\text{--}650^\circ\text{C}$ was due to the lignin decomposition [15]. For the other two biosorbents, there are no distinguishable stages in the curves with almost steady weight loss throughout the tested temperature range. The loss of cellulose and hemicellulose due to acid treatment can be seen as a main reason for this trend. The presence of sulphur containing functional groups on the surface may be the reason for the greater thermal stability of modified biosorbents in comparison to unmodified one [21].

3.2.3. Specific surface area and surface morphology analysis

The specific BET surface areas of unmodified, acid modified and ultrasound-acid modified WHRP were 3.3141 m^2

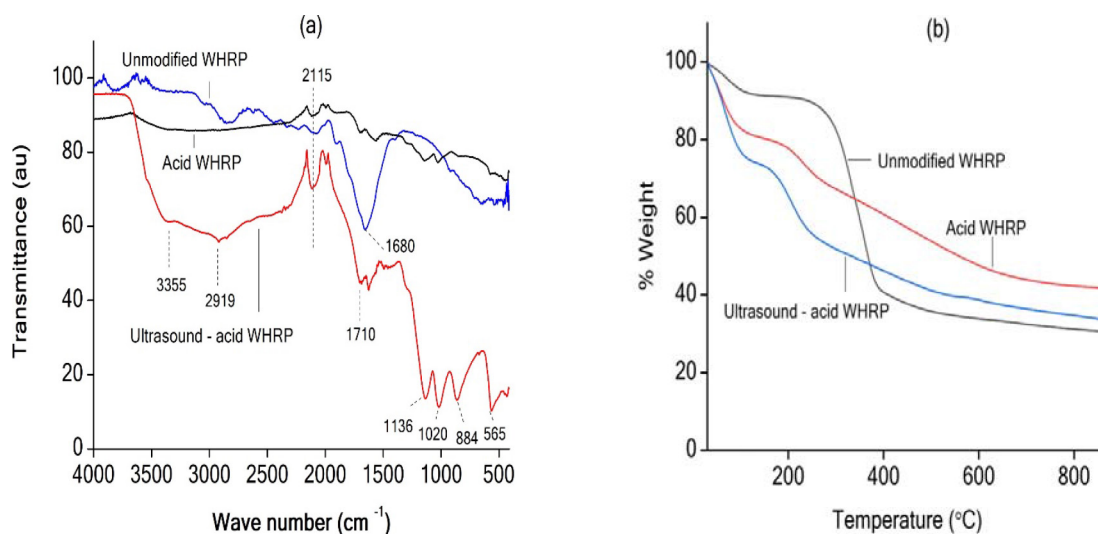


Fig. 2. Characterization of water hyacinth root powders: (a) FT-IR spectra, (b) TGA profiles of unmodified, acid modified and ultrasound-acid modified WHRP.

g^{-1} , $6.1765 \text{ m}^2 \text{ g}^{-1}$ and $6.7388 \text{ m}^2 \text{ g}^{-1}$ respectively. Komy et al. [22] studied the adsorption of Cu^{2+} using *Eichhornia crassipes* (water hyacinth) and the adsorbent surface area was $4.16 \text{ m}^2 \text{ g}^{-1}$. The surface areas of untreated and treated water hyacinth root biomasses were $3.8189 \text{ m}^2 \text{ g}^{-1}$ and $4.1978 \text{ m}^2 \text{ g}^{-1}$ respectively in Muchanyereyi et al. [23]. Hence, the surface areas of water hyacinth root biosorbents prepared in the current investigation are in coherence with the earlier works.

The surface properties of water hyacinth plant biosorbents were analysed using SEM and the corresponding images are shown in Fig. 3. The surfaces of modified WHRP (Figs. 3b, 3c) were coarse, rough and porous compared to that of the unmodified (Fig. 3a). The ultrasound-acid treatment caused more crumbling due to the partial removal of hemicellulose and lignin that interconnects the cellulose fibrils [24] and made the surface more porous. The heterogeneous nature of ultrasound-acid modification can potentially introduce more functional groups on the surface [25]. Although the BET surface areas of modified biosorbents are comparable, the presence of more functional groups on the surface with ultrasound-acid modification can result in increased biosorption capacity.

3.3. Biosorption of 2,4-D

3.3.1. Effect of biosorbent dosage and initial solution pH

Three different dosages of ultrasound-acid modified WHRP (2, 4, 6 g L^{-1}) were used for biosorption studies in 100 mg L^{-1} concentration of 2,4-D solution at native pH. Fig. S1 (supplementary data) shows the percentage removal of 2,4-D for these three biosorbent loadings. The equilibrium removal for 2 g L^{-1} and 4 g L^{-1} biosorbent loadings are 74% and 90% respectively. By increasing the amount of biosorbent, the accessible sites for biosorption increases automatically and culminates towards enhanced biosorption of 2,4-D. The biosorbent dosage of 4 g L^{-1} is sufficient for the 100 mg L^{-1} of 2,4-D as biosorbent loading of 6 g L^{-1} could not increase the equilibrium percentage removal beyond 90. Similar trend was observed for the biosorption of 2,4-D on cotton plant and ash char [26]. The lowered biosorption capacity with 6 g L^{-1} biosorbent dosage might be due to the unavailability of active binding sites on biosorbent with possible aggregation of biosorbent particles. Hence, 4 g L^{-1} biosorbent dosage was chosen as the optimum loading of biosorbent for 100 mg L^{-1} of 2,4-D.

The solution pH can have a prominent effect on ionic interactions between the surface functional groups of biosor-

bent and the adsorbate [4]. The point of zero charge (pH_{PZC}) of ultrasound-acid modified WHRP was estimated as 4.7 and the measured data is presented in Fig. S2 (supplementary data). If the pH of the solution is below the pH_{PZC} of biosorbent, the surface of the biosorbent becomes overall positive in nature and vice versa [27]. As the P^{ka} value of 2,4-D is 2.7 [28], the degree of dissociation of 2,4-D would be high when solution pH is above 2.7. If the pH of the solution in the batch biosorption experiments is between 2.7 and 4.7, the dissociation of 2,4-D with its existence in anionic form coupled with overall positive charge on the surface of biosorbent makes biosorption more feasible. Fig. 4a depicts the biosorption behaviour of ultrasound-acid modified WHRP at different initial solution pH values. At a lower pH value, i.e., 4, the percentage removal of 2,4-D is 91. At initial pH values greater than 4, the removal percentage of 2,4-D was lower than or equal to 61. It might be due to the reduction of overall positive charge on the surface of biosorbent at these pH values. At $\text{pH} = 2$, the non-dissociation of 2,4-D results in lower 2,4-D biosorption. Hence, the optimum value of initial pH of the solution is taken as 4 in the further experiments.

3.3.2. Effect of initial pesticide concentration

The biosorption studies were carried out using the optimal values of biosorbent dosage and pH (4 g L^{-1} and 4 respectively) for different initial concentrations of pesticide (20–180 mg L^{-1}). The results are plotted in Fig. 4b. In the range of 20–100 mg L^{-1} , the increment in initial pesticide concentration has resulted in the increased removal percentage. The percentage removal drastically decreased with the increase in the initial pesticide concentrations beyond 100 mg L^{-1} . The driving force for mass transfer increases in the biosorption experiments with the increase of initial concentration in the range of 20–100 mg L^{-1} . The available active sites present on the biosorbent surface relatively decreases upon increasing the initial concentration beyond the optimum value of initial concentration (100 mg L^{-1}) which can be seen as lowered percentage removal of pesticide [29].

3.4 Biosorption kinetics

The kinetics of 2,4-D biosorption on ultrasound-acid modified WHRP were analysed using pseudo first and pseudo second order kinetic equations.

The linearized form of pseudo first order kinetic model equation can be written as Eq. (3):

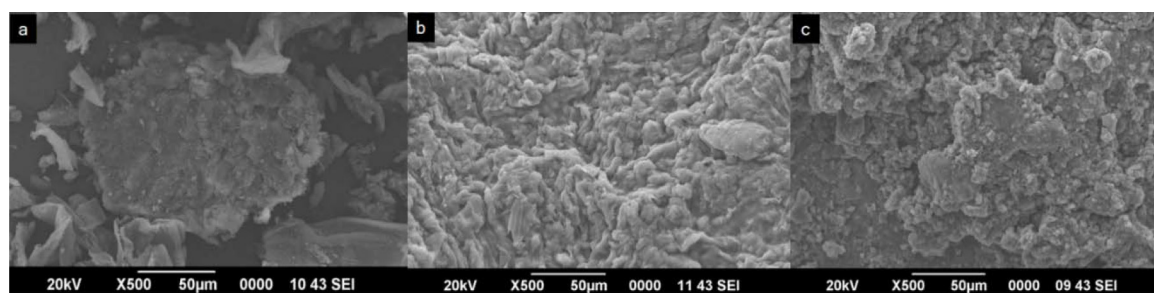


Fig. 3. Scanning electron microscopy images of water hyacinth root powders: (a) Unmodified WHRP, (b) Acid modified WHRP and (c) Ultrasound-acid modified WHRP.

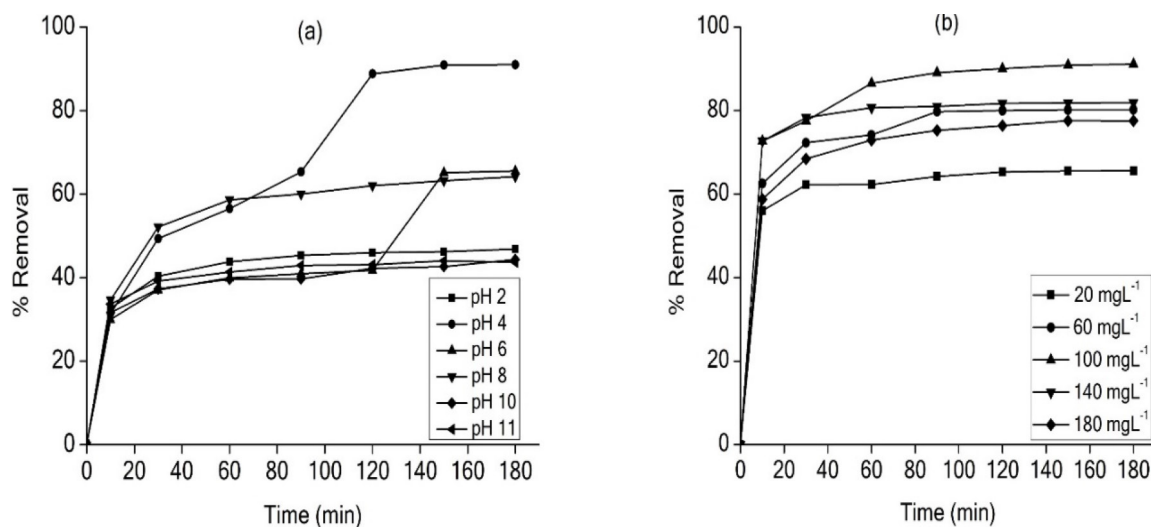


Fig. 4. Effect of parameters on 2,4-D biosorption on ultrasound-acid modified WHRP: (a) Initial solution pH range 2–11, initial concentration 100 mg L⁻¹ (b) Initial solution concentration range 20–180 mg L⁻¹ at pH 4; (biosorbent dosage: 4 g L⁻¹, Exposure time: 3 h, stirring speed: 250 rpm).

$$\log(q_e - q_t) = \log q_e - \frac{k_1 t}{2.303} \quad (3)$$

In this equation, q_e (mg g⁻¹) and q_t (mg g⁻¹) are the amount of 2,4-D adsorbed at equilibrium and time t respectively, and k_1 (min⁻¹) is pseudo first order rate constant of biosorption [9]. The experimental data for the different initial concentrations at a pH of 4 and 4 g L⁻¹ of biosorbent dosage were fitted for the first order pseudo kinetic model. The values of k_1 and q_e were obtained as the slope and intercept of the line between $\log(q_e - q_t)$ and t as shown in Fig. S3 (supplementary data). The values of k_1 , q_e and the correlation coefficient, i.e., R^2 are shown in Table 2. The large deviations between experimental and calculated values of q_e indicate that the pseudo first order kinetic model is inadequate to represent the experimental data.

The linearized form of pseudo second order model is given as (Eq. (4)) [30]:

$$\frac{t}{q_t} = \frac{1}{k_2 q_e^2} + \frac{t}{q_e} \quad (4)$$

where k_2 (g mg⁻¹ h⁻¹) is pseudo second order rate constant [31]. The experimental data was fitted for the linearized form of pseudo second order model. The slope ($1/q_e$) and intercept ($1/k_2 q_e^2$) values of the model equation were estimated (Fig. 5) and the values of k_2 , q_e and R^2 are tabulated in Table 2. For all initial concentration tested, the experimental and calculated values of q_e are comparable and R^2 values are near to unity. The biosorption data of 2,4-D on ultrasound-acid modified WHRP were best fitted to pseudo second order kinetic model, indicating chemisorption type interaction between 2,4-D and the biosorbent. In the earlier studies on the 2,4-D biosorption on activated carbons derived from various lignocellulosic materials [31], nitric acid modified activated carbons [32] and polymer-based activated carbon-polyvinyl alcohol composite [33], the experimental data were best fitted to pseudo second order kinetic model.

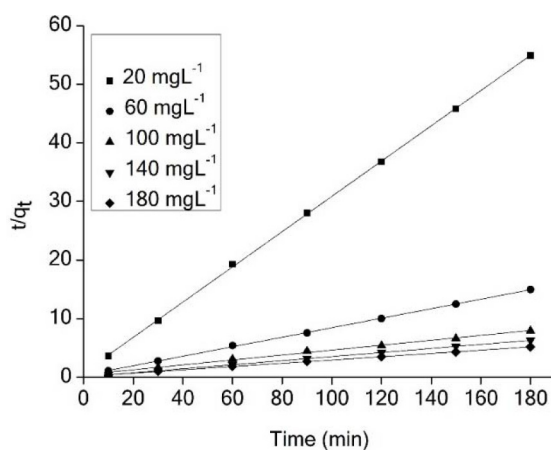


Fig. 5. Pseudo second order kinetic plot for the biosorption of 2,4-D by ultrasound-acid modified WHRP at room temperature.

3.5. Biosorption isotherm models

Through biosorption isotherms, the relation between the specific biosorbed amount or degree of biosorption at the interface and the bulk concentration of the adsorbate at the equilibrium is presented. In the current work, the equilibrium biosorption data of 2,4-D on ultrasound-acid modified WHRP was fitted for four isotherm models namely Langmuir, Freundlich, Halsey and Harkins-Jura. The assumption of homogeneous single layer biosorption is the main feature in the derivation of Langmuir model that no further biosorption on an occupied site of the surface [34,35]. The linear form of the Langmuir model is given as Eq. (5):

$$\frac{C_e}{q_e} = \frac{1}{bQ_0} + \frac{1}{Q_0} c_e \quad (5)$$

where C_e (mg L⁻¹) is the concentration of pesticide in the solution at equilibrium, b (L mg⁻¹) is the Langmuir equilibrium constant related to rate of biosorption and Q_0 (mg g⁻¹)

Table 2
Kinetic parameters for the adsorption of 2,4-D by ultrasound-acid modified WHP at different initial 2,4-D concentrations

Initial conc. (mg L ⁻¹)	q_e , exp. ^a (mg g ⁻¹)	Pseudo-first-order		Pseudo-second-order		Elovich model		Intra particle diffusion model					
		k_1 (min ⁻¹)	q_e , cal. ^b (mg g ⁻¹)	R^2	k_2 (g mg ⁻¹ min ⁻¹)	q_e , cal. ^b (mg g ⁻¹)	R^2	$1/\beta$	$(1/\beta) \times \ln \alpha\beta$	R^2	K_{it} (mg ⁻¹ min ^{1/2})	C	R^2
20	3.30	0.06	4.62	0.73	0.12	3.32	0.99	0.16	2.08	0.92	0.04	2.78	0.83
60	12.02	0.07	17.85	0.82	0.02	12.32	0.99	0.94	7.41	0.94	0.25	9.12	0.85
100	22.74	0.06	66.72	0.69	0.01	23.83	0.99	2.42	10.11	0.94	0.68	14.12	0.98
140	28.66	0.04	7.99	0.89	0.02	28.91	0.99	1.09	23.34	0.91	0.28	25.40	0.79
180	34.89	0.07	84.80	0.74	0.01	35.77	0.99	2.95	20.23	0.97	0.78	25.66	0.87

^a q_e experimental value

^b q_e calculated value

is the maximum biosorption capacity for monolayer formation [36]. The values of Q_0 and b are calculated from the intercept $1/Q_0 b$ and the slope $1/Q_0$ of C_e/q_e versus C_e plot [37] (Fig. 6). The Langmuir constant b , which is the indicative of the energy of biosorption is 0.051 L mg^{-1} (Table 3).

Using the value of b and the range of tested initial concentrations of the adsorbate, a dimensionless equilibrium parameter R_L was proposed to understand the characteristics of the biosorption whether it is favourable or unfavourable etc. [38]. The expression for R_L is given below as Eq. (6) [39]:

$$R_L = \frac{1}{1 + bC_0} \quad (6)$$

The value of R_L specifies the nature of the biosorption as unfavourable ($R_L > 1$), favourable ($0 < R_L < 1$), irreversibility of biosorption ($R_L = 0$) or linear isotherm type ($R_L = 1$) [8]. In the current work, the values of R_L were 0.495 and 0.098 for the minimum and maximum initial concentrations (20 and 180 mg L^{-1}) respectively, which proves the favourable nature of the biosorption. The Langmuir model was satisfactorily fitted with R^2 (0.98) and maximum biosorption capacity value of 40.0 mg g^{-1} .

The Freundlich model can be employed to depict the biosorption on heterogeneous surfaces and multilayer biosorption. The linear form of this isotherm is given as Eq. (7):

$$\log q_e = \log K_f + \frac{1}{n} \log C_e \quad (7)$$

The Freundlich constants K_f and n describe the biosorption capacity and the biosorbent intensity respectively [40].

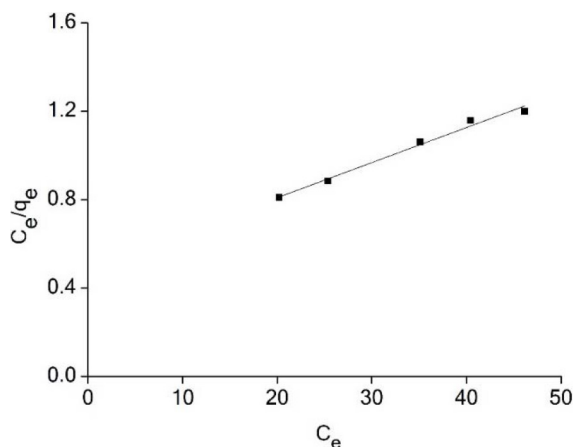


Fig. 6 Langmuir adsorption isotherm plot for the biosorption of 2,4-D by ultrasound-acid modified WHRP at room temperature.

Table 3
Biosorption isotherm parameters for the biosorption of 2,4-D by ultrasound-acid modified WHRP at RT

Langmuir	Freundlich	Halsey	Harkin-Jura
Q_0	n	k_H	A
b	K_f	n_H	B
R^2	R^2	R^2	R^2
40.0	0.96	1.075	32.08
0.051	0.93	-0.960	1.372
0.98	0.91	0.91	0.79

These constants were calculated from the plotted values of $\log q_e$ and $\log C_e$ (Fig. S4, supplementary data) and tabulated in Table 3. The value of n is an indicative of the type of biosorption as linear ($n = 1$), chemisorption ($n < 1$), favorable physisorption ($n > 1$) [41]. From the fitted data, the value of R^2 was found to be 0.91 indicating non-suitability of the Freundlich model for the representation of the biosorption equilibrium data.

Halsey isotherm model is used to represent multilayer biosorption on the heterogeneous surfaces. The linear form of Halsey model can be written as Eq. (8):

$$\ln q_e = \frac{1}{n_H} \ln K_H - \frac{1}{n_H} \ln C_e \quad (8)$$

where K_H and n_H are Halsey's isotherm constants. They were calculated from the slope and intercept of the fitted line of $\ln q_e$ vs. $\ln C_e$ [42] (Fig. S5, supplementary data). The values of the parameters are tabulated in Table 3. The R^2 value was 0.91 suggesting the absence of multilayer biosorption. The Harkin-Jura (H-J) Isotherm is used to analyse the existence of heterogeneous pore distribution. The linear form of H-J model can be represented as (Eq. (9)) [42,43]:

$$\frac{1}{q_e^2} = \frac{B}{A} - \frac{1}{A} \log C_e \quad (9)$$

where A and B are H-J constants and they can be calculated from the slope and intercept of the linear plot of $1/q_e^2$ vs. $\log C_e$ (Fig. S6, supplementary data). The R^2 value of fitted data was found to be 0.79 (Table 3) indicating the non-existence of heterogeneous pore distribution and multi-layered biosorption on the surface.

3.6. Biosorption mechanism

3.6.1. Electrostatic interaction

For the purpose of understanding biosorption mechanism, it is essential to analyse the electrostatic interaction between 2,4-D and the surface functional groups of the biosorbent. The ionic form of 2,4-D in water solution above p^{ka} value of 2.7 can be represented as Eq. (10) [32]:



Since the surface of the biosorbent is neutral at the point of zero charge ($pH_{pZC} = 4.7$), the deprotonated 2,4-D for pH values between 2.7 and 4.7 electrostatically adheres the surface of the biosorbent. This is the reason for maximum biosorption removal capacity observed at $pH = 4$. Hence, solution pH is a critical parameter in the biosorption of 2,4-D. Also, the density of functional groups containing sulphur is high in case of ultrasound-acid modified WHRP in comparison to acid modified one as shown in the FT-IR analysis in Fig. 2a.

3.6.2. Elovich model

Elovich model is one of the kinetic models that is used to model the kinetics of chemisorption and slow biosorption rate processes. The biosorption rate decreases exponentially with the increase in the amount of adsorbed molecules in

this model [44]. The linear form of the model is given as Eq. (11):

$$q_t = \frac{1}{\beta} \ln \alpha \beta + \frac{1}{\beta} \ln t \quad (11)$$

where α ($\text{mg g}^{-1} \text{min}^{-1}$) is the initial biosorption rate and β (g mg^{-1}) is associated with the surface coverage and energy for chemisorption [39]. The value of $1/\beta$ represents the number of accessible sites for biosorption and $1/\beta (\ln(\alpha\beta))$ portrays the biosorption quantity when $\ln t$ is equal to zero [36,45]. The values of the above parameters were obtained from the slope and intercept of the linear plot of q_t versus $\ln t$ as shown in Fig. S7 (supplementary data) [37]. The values of α and β are given in Table 2. The R^2 values were in the range of 0.91–0.97 for the tested initial concentrations of pesticide suggesting chemisorption of 2,4-D by ultrasound-acid modified biosorbent.

3.6.3. Weber's intra particle diffusion model

To understand the mechanism of diffusion, the biosorption data was fitted for Weber's intra particle diffusion model. Note that at higher agitation rates, the adsorbate transfer from the bulk onto the biosorbent surface is not rate limiting due to rapidity. Nevertheless, the intra particle diffusion of the adsorbate would be much slower in comparison to its transfer from the bulk to the surface at higher agitation rates. Hence, the intra particle diffusion becomes rate limiting step in such situations. The Weber's intra particle model is expressed as Eq. (12) [46]:

$$q_t = K_{di} t^{0.5} + C \quad (12)$$

where K_{di} is the intra particle diffusion rate constant ($\text{mg g}^{-1} \text{min}^{1/2}$) and C is the thickness of the boundary layer and can be obtained from the intercept of q_t versus $t^{0.5}$ plot. A larger value of C indicates more efficient boundary layer for mass transfer [47]. The experimental data is plotted in Fig. 7a and three different regions of varying slopes can be seen in the

figure. The biosorption in the region I is very rapid due to instantaneous biosorption at the external surfaces. The lines of the regions II and III do not pass through origin. This trends signify varying mass transfer rates with respect to time confirming intra particle diffusion and also the existence of rate limiting mechanisms other than intra particle diffusion [48]. Similar results were described in Hameed et al. [5] for the biosorption of 2,4-D using activated carbon from date stones. The values of K_{di} , C and R^2 are given in Table 2.

3.6.4. Boyd's intra particle diffusion model

Boyd's diffusion model was applied in various biosorption studies earlier [49] as it helps to find out the rate-controlling step in biosorption. The Boyd model is given in Eq. (13) as:

$$F(t) = \frac{q_t}{q_e} = 1 - \left(\frac{6}{\pi^2} \right) \sum_{n=1}^{\infty} \frac{1}{n^2} \exp(-n^2 Bt) \quad (13)$$

where $F(t)$ is the fractional achievement of equilibrium at time t , and Bt is a function of $F(t)$ [47]. q_t and q_e are the adsorbate uptake (mg g^{-1}) at time t and equilibrium respectively. For Eq. (14), with the application of Fourier transform and integration for $F(t) > 0.85$ and $F(t) \leq 0.85$, the expressions for Bt can be obtained as Eq. (14) and Eq. (15) respectively [50].

$$Bt = 0.4977 - \ln(1 - F(t)) \quad \text{for } > 0.85, \quad (14)$$

$$Bt = \left(\sqrt{\pi} - \sqrt{\pi - \left(\frac{\pi^2 F(t)}{3} \right)} \right)^2 \quad \text{for } \leq 0.85, \quad (15)$$

If the intra particle diffusion is the rate controlling step, the relation of Bt versus time t (min) is linear passing through origin. Otherwise, film diffusion is considered as rate controlling step [51]. In the plot of Bt versus t shown

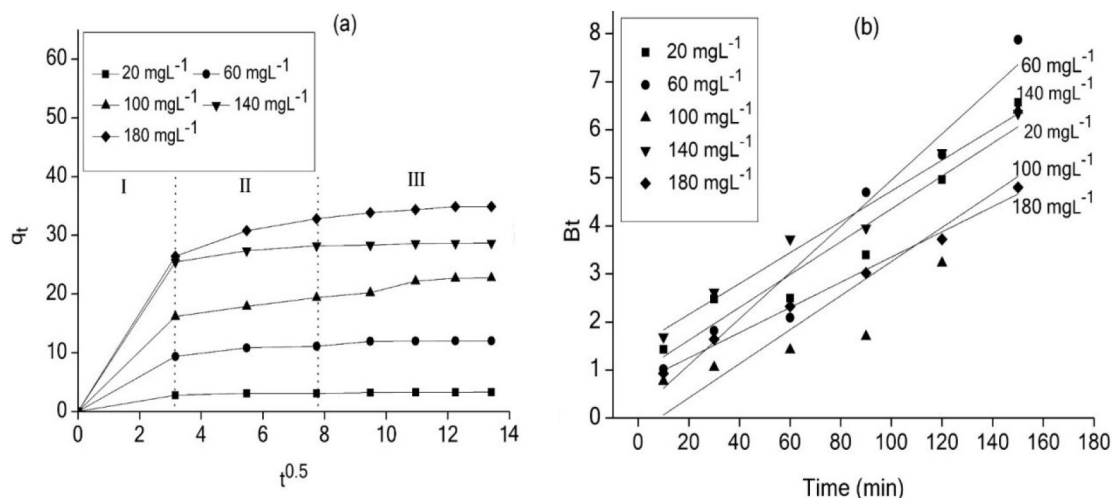


Fig. 7. Intra particle diffusion models for the adsorption of 2,4-D by ultrasound-acid modified WHRP at room temperature, (a) Weber's intra particle diffusion model, (b) Boyd's intra particle diffusion model (biosorbent dosage: 4 g L^{-1} , Exposure time: 3 h, stirring speed: 250 rpm, initial 2,4-D solution concentration: 20–180 mg L^{-1} , pH 4).

in Fig. 7b, the relationships are not linear for all initial concentrations. It indicates that the rate limiting step is the film-diffusion as per this model.

3.7. Desorption studies

After the biosorption of 2,4-D on the ultrasound-acid modified biosorbent, the desorption studies were carried out with NaOH as desorption agent. The desorption percentages were calculated using the formula given in Eq. (16) [52].

$$\text{Desorption \%} = \frac{\text{amount of ions desorbed}}{\text{amount of ions adsorbed}} \times 100 \quad (16)$$

For the desorption, the 2,4-D loaded biosorbent was treated with 50 ml of 0.1 M NaOH solution (90 min stirring at native *pH* and room temperature). The supernatants were collected and analysed for the concentration of 2,4-D. Desorption percentages were found to be 40.18, 23.45 and 12.64 respectively for the three consecutive biosorption-desorption cycles. The studies pertaining to desorption such as selection of agent, method and kinetics are very essential which form our future study.

4. Conclusion

In the current investigation, water hyacinth root powder (WHRP) both in unmodified and modified forms were analysed for the 2,4-D removal from water. Among the different type of modifications employed, ultrasound-acid modification (6% H₂SO₄ solution, sonication for 30 min) of the WHRP exhibited maximum affinity for the pesticide biosorption. The ultrasound-acid modification of the biosorbent resulted in enhanced porosity with the incorporation of surface functional groups suitable for maximum 2,4-D removal (91%). The optimum values of *pH*, biosorbent dosage and initial solution concentration were found to be 4.0 and 4 g L⁻¹ for 100 mg L⁻¹ 2,4-D solution. The isotherm studies indicated mono layered biosorption of 2,4-D on the ultrasound-acid treated biosorbent with the equilibrium data best fitted for Langmuir model. Among the different kinetic models tested, the biosorption data was best fitted to pseudo second order kinetic model. The intra particle and film diffusion limitations for the biosorption of pesticide were confirmed using two well-known intra particle diffusion models namely Weber and Boyd. Since water hyacinth is seen as a serious threat to native species in water bodies, devising suitable routes for converting this waste biomass into valuable products is thus necessary. In this work, ultrasound-acid treated water hyacinth root powder biomass is shown to be an efficient biosorbent for the removal of 2,4-D from its aqueous solution.

Acknowledgement

The partial financial support by Technical Education Quality Improvement Programme (TEQIP) - Phase II, National Institute of Technology Calicut (NITC/TEQIP-II/R&D/2014) is gratefully acknowledged.

Symbols

2,4-D	—	2,4-dichlorophenoxy acetic acid
<i>A</i>	—	H-J constant
<i>B</i>	—	H-J constant
<i>b</i>	—	Langmuir equilibrium constant (L mg ⁻¹)
<i>Bt</i>	—	A function of <i>F(t)</i>
<i>C</i>	—	Thickness of boundary layer in intraparticle diffusion model
<i>C_e</i>	—	Solution concentration at equilibrium (mg L ⁻¹)
<i>C₀</i>	—	Initial solution concentration (mg L ⁻¹)
<i>F(t)</i>	—	Fractional achievement of equilibrium in Boyd model
<i>k₁</i>	—	Pseudo first order rate constant (min ⁻¹)
<i>k₂</i>	—	Pseudo second order rate constant (g mg ⁻¹ h ⁻¹)
<i>K_{di}</i>	—	Intraparticle diffusion rate constant (mg g ⁻¹ min ^{1/2})
<i>K_f</i>	—	Freundlich constant (L g ⁻¹)
<i>K_H</i>	—	Halsey's isotherm constant
<i>n</i>	—	Freundlich exponent
<i>n_H</i>	—	Halsey's isotherm constant
<i>Q₀</i>	—	Maximum adsorption capacity (mg g ⁻¹)
<i>q_e</i>	—	Amount of pesticide adsorbed (mg g ⁻¹) at equilibrium
<i>q_t</i>	—	Amount of pesticide adsorbed (mg g ⁻¹) at <i>t</i>
<i>R%</i>	—	Removal percentage
<i>R²</i>	—	Correlation coefficient
<i>R_L</i>	—	Langmuir adsorption isotherm equilibrium parameter
<i>V</i>	—	Volume of 2, 4-D solution (mL)
<i>W</i>	—	Amount of biosorbent (g)
WH	—	Water hyacinth
WHRP	—	Water hyacinth root powder
<i>α</i>	—	Initial biosorption rate (mg g ⁻¹ min ⁻¹) in Elovich model
<i>β</i>	—	Surface coverage and energy for chemisorption (g mg ⁻¹)

References

- [1] V.O Njoku, M. Asif, B.H. Hameed, 2,4-dichlorophenoxyacetic acid adsorption onto coconut shell-activated carbon: isotherm and kinetic modelling, *Desal. Water Treat.*, 55(1) (2015) 1–10.
- [2] E. Bazrafshan, F.K. Mostafapour, H. Faridi, M. Farzadkia, S. Sargazi, A. Sohrabi, Removal of 2,4-dichlorophenoxyacetic acid (2,4-D) from aqueous environments using single-walled carbon nanotubes, *Health Scope.*, 2(1) (2013) 39–46.
- [3] Y.F. Chao, P.C. Chen, S.L. Wang, Adsorption of 2,4-D on Mg/Al-NO₃ layered double hydroxides with varying layer charge density, *Appl. Clay Sci.*, 40 (2008) 193–200.
- [4] M. Dehghani, S. Nasser, M. Karamimanesh, Removal of 2,4-dichlorophenoxyacetic acid (2,4-D) herbicide in the aqueous phase using modified granular activated carbon, *J. Environ. Health Sci. Eng.*, 12(28) (2014) 1–10.
- [5] B.H. Hameed, J.M. Salman, A.L. Ahmad, Adsorption isotherm and kinetic modelling of 2,4-D pesticide on activated carbon derived from date stones, *J. Hazard. Mater.*, 163(1) (2009) 121–126.
- [6] E. Suganya, S. Rangabhashiyam, A.V. Lity, N. Selvaraju, Removal of hexavalent chromium from aqueous solution by a novel biosorbent *Caryota urens* seeds: equilibrium and kinetic studies, *Desal. Water Treat.*, 57(50) (2016) 23940–23950.

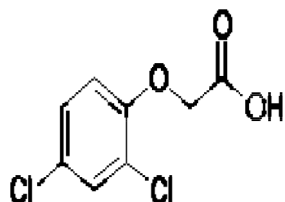
- [7] S. Rangabhashiyam, M.S.G. Nandagopal, E. Nakkeeran, N. Selvaraju, Adsorption of hexavalent chromium from synthetic and electroplating effluent on chemically modified Swietenia mahagoni shell in a packed bed column, *Environ. Monit. Assess.*, 188(7) (2016) 411.
- [8] J.M. Salman, B.H. Hameed, Adsorption of 2,4-dichlorophenoxyacetic acid and carbofuran pesticides onto granular activated carbon, *Desalination*, 256 (2010) 129–135.
- [9] V. Nair, R. Vinu, Peroxide-assisted microwave activation of pyrolysis char for adsorption of dyes from wastewater, *Bioresour. Technol.*, 216 (2016) 511–519.
- [10] F.T. Kanga, Modeling adsorption mechanism of Paraquat onto Ayous (*Triplochiton scleroxylon*) wood sawdust, *Appl. Water Sci.*, 9(1) (2019) 1–7.
- [11] E.E. Priya, P.S. Selvan, Water hyacinth (*Eichhornia crassipes*)-An efficient and economic adsorbent for textile effluent treatment-A review, *Arab. J. Chem.*, 10(2) (2014) S3548–S3558.
- [12] I.A.H. Schneider, J. Rubio, M. Misra, R.W. Smith, *Eichhornia Crassipes* as biosorbent for heavy metal ions, *Miner. Eng.*, 8(9) (1995) 979–988.
- [13] K.S. Low, C.K. Lee, K.K. Tan, Biosorption of basic dyes by Water hyacinth roots, *Bioresour. Technol.*, 52(1) (1995) 79–83.
- [14] K. Yang, Y. Jiang, J. Yang, D. Lin, Correlations and adsorption mechanisms of aromatic compounds on biochars produced from various biomass at 700°C, *Environ. Pollut.*, 233 (2018) 64–70.
- [15] B. Girisuta, B. Danon, R. Manurung, L.P.B.M. Janssen, H.J. Heeres, Experimental and kinetic modelling studies on the acid-catalysed hydrolysis of the water hyacinth plant to levulinic acid, *Bioresour. Technol.*, 99(17) (2008) 8367–8375.
- [16] V.O. Njoku, B.H. Hameed, Preparation and characterization of activated carbon from corncob by chemical activation with H_3PO_4 for 2,4-dichlorophenoxyacetic acid adsorption, *Chem. Eng. J.*, 173(2) (2011) 391–399.
- [17] R. Elangovan, L. Philip, K. Chandraraj, Biosorption of chromium species by aquatic weeds: Kinetics and mechanism studies, *J. Hazard. Mater.*, 152(1) (2008) 100–112.
- [18] Y. Miller, G.M. Chaban, R.B. Gerber, Ab Initio vibrational calculations for H_2SO_4 and $H_2SO_4 \cdot H_2O$: Spectroscopy and the nature of the anharmonic couplings, *J. Phys. Chem. A.*, 109(29) (2005) 6565–6574.
- [19] V. Nair, A. Panigrahy, R. Vinu, Development of novel chitosan-lignin composites for adsorption of dyes and metal ions from wastewater, *Chem. Eng. J.*, 254 (2014) 491–502.
- [20] R. Han, L. Zhang, C. Song, M. Zhang, H. Zhu, L. Zhang, Characterization of modified wheat straw, kinetic and equilibrium study about copper ion and methylene blue adsorption in batch mode, *Carbohydr. Polym.*, 79(4) (2010) 1140–1149.
- [21] N. Bujang, M.N.M. Rodhi, M. Musa, F. Subari, N. Idris, N.S.M. Makhtar, K.H.K. Hamid, Effect of dilute sulfuric acid hydrolysis of coconut dregs on chemical and thermal properties, *Procedia Eng.*, 68 (2013) 372–378.
- [22] Z.R. Komy, W.H. Abdelraheem, N.M. Ismail, Biosorption of Cu^{2+} by *Eichhornia crassipes*: Physicochemical characterization, biosorption modelling and mechanism, *J. King Saud Univ.-Sci.*, 25(1) (2013) 47–56.
- [23] N.M. Muchanyereyi, J. Kugara, M.F. Zaranyika, Thermodynamic parameters for the adsorption of volatile n-alkane hydrocarbons on water hyacinth (*Eichhornia crassipes*) root biomass: Effect of organic solvent and mineral acid treatment, *Afr. J. Environ. Sci. Technol.*, 9(3) (2015) 282–291.
- [24] N.M. Muchanyereyi, J. Kugara, M.F. Zaranyika, Surface composition and surface properties of water hyacinth (*Eichhornia crassipes*) root biomass: Effect of mineral acid and organic solvent treatment, *Afr. J. Biotechnol.*, 15 (2016) 897–909.
- [25] N. Saranya, E. Nakkeeran, S. Shrihari, N. Selvaraju, Equilibrium and kinetic studies of hexavalent chromium removal using a novel biosorbent: *Ruellia Patula* Jacq, *Arab. J. Sci. Eng.*, 42(4) (2017) 1545–1557.
- [26] S.N. Trivedi, R.A. Kharkar, S.A. Mandavgane, Utilization of cotton plant ash and char for removal of 2,4-dichlorophenoxyacetic acid, *Resour. Technol.*, 2 (2016) S39–S46.
- [27] D. Borah, S. Satokawa, S. Kato, T. Kojima, Surface-modified carbon black for As (V) removal, *J. Colloid Interface Sci.*, 319(1) (2008) 53–62.
- [28] J.P. Kearns, L.S. Wellborn, R.S. Summers, D.R. Knappe, 2,4-D adsorption to biochars: Effect of preparation conditions on equilibrium adsorption capacity and comparison with commercial activated carbon literature data, *Water Res.*, 62 (2014) 20–28.
- [29] D. Pathania, S. Sharma, P. Singh, Removal of methylene blue by adsorption onto activated carbon developed from *Ficus carica* bast, *Arab. J. Chem.*, 10(1) (2017) S1445–S1451.
- [30] G. Annadurai, L.Y. Ling, J.F. Lee, Adsorption of reactive dye from an aqueous solution by chitosan: isotherm, kinetic and thermodynamic analysis, *J. Hazard. Mater.*, 152(1) (2008) 337–346.
- [31] B. Doczekalska, K. Kusmierk, A. Swiatkowski, M. Bartkowiak, Adsorption of 2,4-dichlorophenoxyacetic acid and 4-chloro-2-methylphenoxyacetic acid onto activated carbons derived from various lignocellulosic materials, *J. Environ. Sci. Health B.*, 53(5) (2018) 290–297.
- [32] Q. Li, J. Sun, T. Ren, L. Guo, Z. Yang, Q. Yang, H. Chen, Adsorption mechanism of 2,4-dichlorophenoxyacetic acid onto Nitric acid modified activated carbon fiber, *Environ. Technol.*, 39(7) (2017) 895–906.
- [33] M.A. Lelifajri, S. Nawi, S. Sabar, W.I. Nawawi, Preparation of immobilized activated carbon-polyvinyl alcohol composite for the adsorptive removal of 2,4-dichlorophenoxyacetic acid, *J. Water Process Eng.*, 25 (2018) 269–277.
- [34] B.H. Hameed, Equilibrium and kinetic studies of methyl violet sorption by agricultural waste, *J. Hazard. Mater.*, 154(1–3) (2008) 204–212.
- [35] I. Langmuir, The adsorption of gases on plane surfaces of glass, mica and platinum, *J. Am. Chem. Soc.*, 40 (1918) 1361–1368.
- [36] T.E. Khalil, A.E. Dissouky, S. Rizk, Equilibrium and kinetic studies on Pb^{2+} , Cd^{2+} , Cu^{2+} and Ni^{2+} adsorption from aqueous solution by Resin 2, 2'-(ethylenedithio)diethanol immobilized amberlite XAD-16 (EDTDE-AXAD-16) with chlorosulphonic acid, *J. Mol. Liq.*, 219 (2016) 533–546.
- [37] I.A.W. Tan, A.L. Ahmad, B.H. Hameed, Adsorption isotherms, kinetics, thermodynamics and desorption studies of 2,4,6-trichlorophenol on oil palm empty fruit bunch-based activated carbon, *J. Hazard. Mater.*, 164(2–3) (2009) 473–482.
- [38] M. Rafatullah, O. Sulaiman, R. Hashim, A. Ahmad, Adsorption of copper (II), chromium (III), nickel (II) and lead (II) ions from aqueous solutions by Meranti sawdust, *J. Hazard. Mater.*, 170(2–3) (2009) 969–977.
- [39] R.L. Liu, Y. Liu, X.Y. Zhou, Z.Q. Zhang, J. Zhang, F.Q. Dang, Biomass-derived highly porous functional carbon fabricated by using a free-standing template for efficient removal of methylene blue, *Bioresour. Technol.*, 154 (2014) 138–147.
- [40] A.I. Adeogun, R.B. Balakrishnan, Kinetics, isothermal and thermodynamics studies of electro coagulation removal of basic dye Rhodamine B from aqueous solution using steel electrodes, *Appl. Water Sci.*, 7(4) (2017) 1711–1723.
- [41] S. Sadaf, H.N. Bhatti, S. Ali, K. Rehman, Removal of Indosol Turquoise FBL dye from aqueous solution by bagasse, a low cost agricultural waste: batch and column study, *Desal. Water Treat.*, 52(1–3) (2014) 184–198.
- [42] C. Solisio, S. Al Arni, A. Converti, Adsorption of inorganic mercury from aqueous solutions onto dry biomass of *Chlorella vulgaris*: Kinetic and isotherm study, *Environ. Technol.*, 40(5) (2017) 1–9.
- [43] A.M.M. Vargas, A.L. Cazetta, M.H. Kunita, T.L. Silva, V.C. Almeida, Adsorption of methylene blue on activated carbon produced from flamboyant pods (*Delonix regia*): Study of adsorption isotherms and kinetic models, *Chem. Eng. J.*, 168 (2011) 722–730.
- [44] A.B. Perez-Marin, V.M. Zapata, J.F. Ortuno, M. Aguilar, J. Saes, M. Llorens, Removal of cadmium from aqueous solutions by adsorption onto orange waste, *J. Hazard. Mater.*, 139(1) (2007) 122–131.
- [45] T. Zheng, Q. Wang, Z. Shi, Z. Zhang, Y. Ma, Microwave regeneration of spent activated carbon for the treatment of ester-containing wastewater, *RSC Adv.*, 6(65) (2016) 60815–60825.

- [46] A. Alahabadi, G. Moussavi, Preparation, characterization and atrazine adsorption potential of mesoporous carbonate-induced activated biochar (CAB) from *Calligonum comosum* biomass: Parametric experiments and kinetics, equilibrium and thermodynamic modelling, *J. Mol. Liq.*, 242 (2016) 40–52.
- [47] D. Banerjee, U. Sarkar, S. Chakraborty, D. Roy, Removal of a cationic bisbiguanide using functionalized activated carbons (FACs), *Process Saf. Environ.*, 92(6) (2013) 957–972.
- [48] L.S. Rocha, A. Almeida, C. Nunes, B. Henriques, M.A. Coimbra, C.B. Lopes, C.M. Silva, A.C. Duarte, E. Pereira, Simple and effective chitosan based films for the removal of Hg from waters: Equilibrium, kinetic and ionic competition, *Chem. Eng. J.*, 300 (2016) 217–229.
- [49] R.M.C. Viegas, M. Campinas, H. Costa, M.J. Rosa, How do the HSDM and Boyd's model compare for estimating intra particle diffusion coefficients in adsorption processes, *Adsorption*, 20(5–6) (2014) 737–746.
- [50] E.G. Deze, S.K. Papageorgiou, E.P. Favvas, F.K. Katsaros, Porous alginate aerogel beads for effective and rapid heavy metal sorption from aqueous solutions: Effect of porosity in Cu^{2+} and Cd^{2+} ion sorption, *Chem. Eng. J.*, 209 (2012) 537–546.
- [51] G.F. Malash, M.I. El-Khaiary, Piecewise linear regression: A statistical method for the analysis of experimental adsorption data by the intra particle diffusion models, *Chem. Eng. J.*, 163(3) (2010) 256–263.
- [52] V.K. Gupta, A. Rastogi, Sorption and desorption studies of chromium (VI) from nonviable cyanobacterium *Nostoc muscorum* biomass, *J. Hazard. Mater.*, 154(1–3) (2008) 347–354.

Supplementary Data

Table S1
General physicochemical characteristics of 2,4-D

2,4-D	General characteristics
Structural formula	<ul style="list-style-type: none"> • Molecular formula: $C_8H_6Cl_2O_3$ • Molecular weight: $221.04 \text{ g mol}^{-1}$ • IUPAC: 2,4-dichlorophenoxy acetic acid • White to yellow powder • Melting point: 140.5°C • Solubility in Water - 900 mg L^{-1} • Carcinogenic, kidney failure and skeletal muscle damage

Table S2
FTIR analysis of unmodified, acid modified and ultrasound-acid modified WHRP

Wave number (cm^{-1})*	Bond stretches	(a)	(b)	(c)
3520–3250	OH and NH (3355 cm^{-1})	✓	✓	✓
2990–2850	CH (2919 cm^{-1})	✓	✓	✓
2140–2100	C=C (2155 cm^{-1})	✓	✓	✓
1710–1690	C=O, carboxylic (1710 cm^{-1})	✓	✓	✓
1680–1620	C=O (1680 cm^{-1})	✓	✓	✓
1149–1118	S-OH bend (1136 cm^{-1})	×	✓	✓
1060–1025	C-O (1020 cm^{-1})	×	✓	✓
917–867	S(OH) ₂ asymmetric (884 cm^{-1})	×		
		×	✓	
635–536	O-S=O (565 cm^{-1})	×	×	✓

*(a) unmodified, (b) acid modified & (c) ultrasound-acid modified WHRP

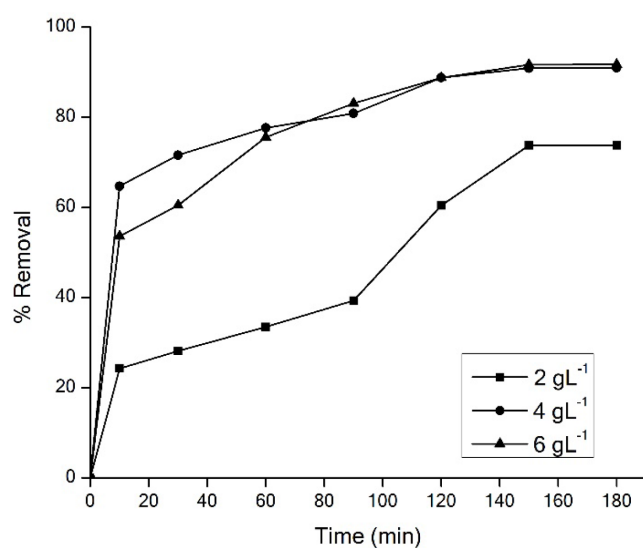
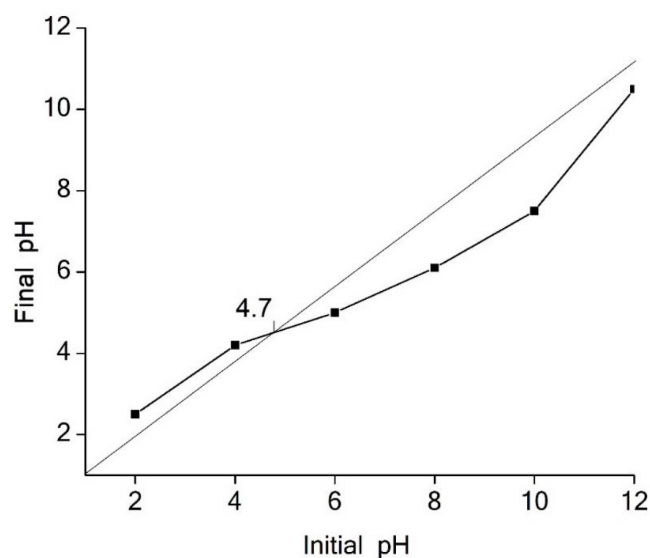
Fig. S1. Effect of biosorbent dosage on 2,4-D biosorption by ultrasound-acid modified WHRP (initial 2,4-D solution concentration: 100 mg L^{-1} , Contact time: 3 h, agitation speed: 250 rpm at native pH, biosorbent dosage: 2–6 g L^{-1}).

Fig. S2. Point of zero charge of ultrasound-acid modified biosorbent (pH 2–12 in 0.1 M NaCl solution for 48 h).

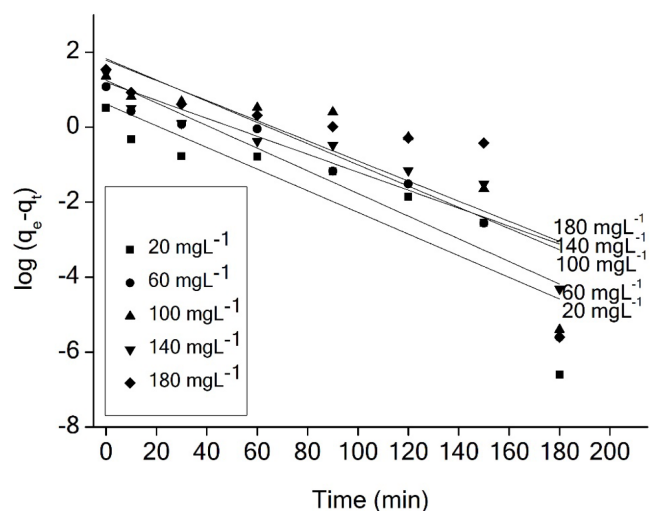


Fig. S3. Pseudo first order kinetic plot for the biosorption of 2,4-D by ultrasound-acid modified WHRP at room temperature.

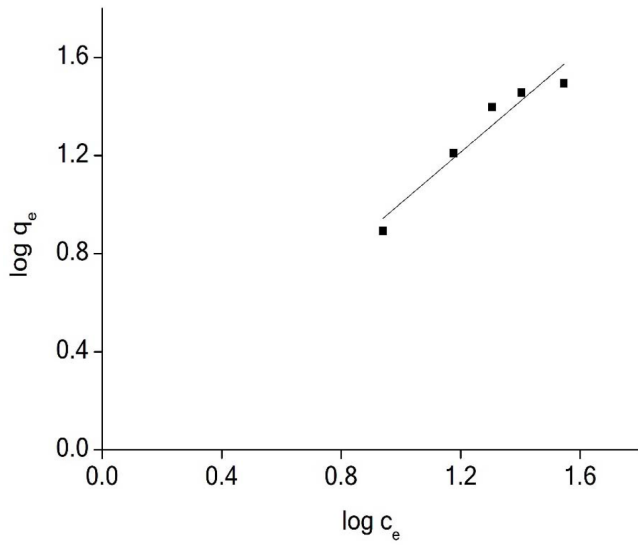


Fig. S4. Freundlich adsorption isotherm plot for the biosorption of 2,4-D by ultrasound-acid modified WHRP at room temperature.

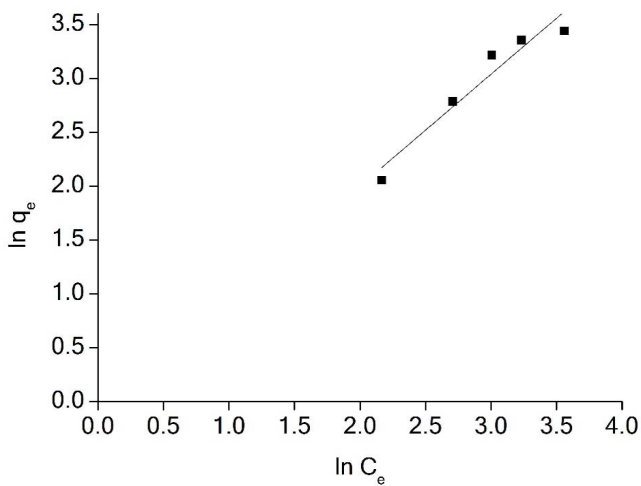


Fig. S5. Halsey isotherm model plot for the biosorption of 2,4-D by ultrasound-acid modified WHRP at room temperature.

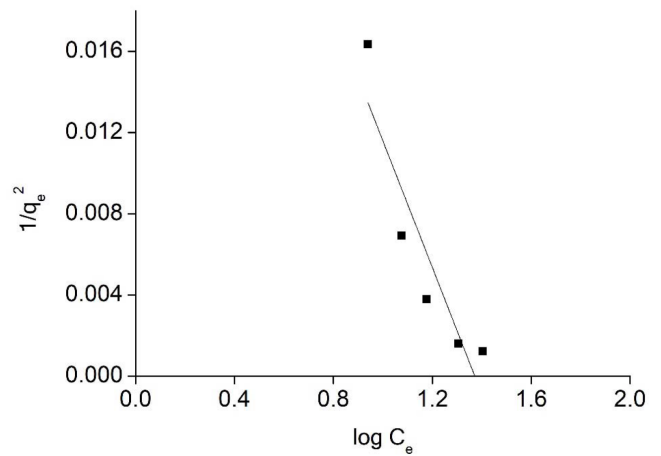


Fig. S6. Harkin-Jura isotherm model plot for the biosorption of 2,4-D by ultrasound-acid modified WHRP at room temperature.

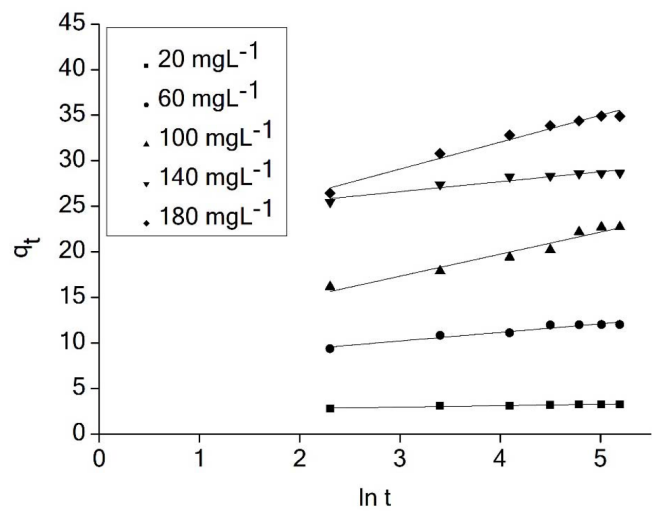


Fig. S7. Elovich model plot for the biosorption of 2,4-D by ultrasound-acid modified WHRP at room temperature.